



Research paper

Solid-state Al-air battery with an ethanol gel electrolyte

Yifei Wang^{a,b,*}, Wending Pan^b, Kee Wah Leong^b, Shijing Luo^b, Xiaolong Zhao^b,
Dennis Y.C. Leung^{b,**}

^a School of Mechanical Engineering and Automation, Harbin Institute of Technology, Shenzhen, China

^b Department of Mechanical Engineering, The University of Hong Kong, Hong Kong, China

Received 15 March 2021; revised 19 April 2021; accepted 24 May 2021

Available online ■ ■ ■

Abstract

Hydrogel electrolyte is especially suitable for solid-state Al-air batteries targeted for various portable applications, which may, however, lead to continuous Al corrosion during battery standby. To tackle this issue, an ethanol gel electrolyte is developed for Al-air battery for the first time in this work, by using KOH as solute and polyethylene oxide as gelling agent. The ethanol gel is found to effectively inhibit Al corrosion compared with the water gel counterpart, leading to stable Al storage. When assembled into an Al-air battery, the ethanol gel electrolyte achieves a much improved discharge lifetime and specific capacity, which are 5.3 and 4.1 times of the water gel electrolyte at 0.1 mA cm⁻², respectively. By studying the gel properties, it is found that a lower ethanol purity can improve the battery power output, but at the price of decreased discharge efficiency. On the contrary, a higher polymer concentration will decrease the power output, but can bring extra benefit to the discharge efficiency. As for the gel thickness, a moderate value of 1 mm is preferred to balance the power output and energy efficiency. Finally, to cater the increasing market of flexible electronics, a flexible Al-air battery is developed by impregnating the ethanol gel into a paper substrate, which can function normally even under serious deformation or damage.

© 2021, Institute of Process Engineering, Chinese Academy of Sciences. Publishing services by Elsevier B.V. on behalf of KeAi Communications Co., Ltd. This is an open access article under the CC BY-NC-ND license (<http://creativecommons.org/licenses/by-nc-nd/4.0/>).

Keywords: Al-air battery; Gel electrolyte; Ethanol gel; Al corrosion; Polyethylene oxide

1. Introduction

Metal-air battery employs a metal anode and an air-breathing cathode for electricity generation, which combines the advantages of conventional battery technologies with the fuel cell [1]. In general, the metal anode provides free electrons during operation, which is regarded as a solid fuel without the need for complex fuel delivery. The ambient air works as oxidant via the air-breathing cathode, which does not need to be stored inside the battery. Consequently, the metal-

air battery achieves both simplified system and improved energy density compared with fuel cells and conventional batteries, which is especially promising for portable electronics.

Among various metal-air batteries, the Al-air battery is getting more and more attention because of its distinct advantages in energy density, fabrication cost and power output [2]. Al has a high specific energy of 8.1 kWh kg⁻¹, which is only next to Li among all common metals. In addition, Al is relatively low-cost because of its large reserve in the earth crust (8.23% by mass) [3], which is therefore widely utilized as anode material or cathode current collector in metal ion batteries [4–6]. Furthermore, Al is electrochemically active when in contact with alkaline electrolyte, ensuring a high power density of several hundred mW cm⁻² [7]. Therefore, it is believed to have a wide application prospect in fields of stationary backup powers, electric vehicles and portable electronics.

* Corresponding author. School of Mechanical Engineering and Automation, Harbin Institute of Technology, Shenzhen, China.

** Corresponding author.

E-mail addresses: wanglfei@connect.hku.hk (Y. Wang), ytleung@hku.hk (D.Y.C. Leung).

<https://doi.org/10.1016/j.gee.2021.05.011>

2468-0257/© 2021, Institute of Process Engineering, Chinese Academy of Sciences. Publishing services by Elsevier B.V. on behalf of KeAi Communications Co., Ltd. This is an open access article under the CC BY-NC-ND license (<http://creativecommons.org/licenses/by-nc-nd/4.0/>).

Please cite this article as: Y. Wang et al., Solid-state Al-air battery with an ethanol gel electrolyte, Green Energy & Environment, <https://doi.org/10.1016/j.gee.2021.05.011>

Nevertheless, the current Al-air battery is haunted by a notorious problem called the Al self-corrosion, which is mainly due to the instability of Al in strong alkaline environment. This problem leads to many obstacles towards its practical application, such as low energy efficiency, short shelf life and safety concerns. For relatively large battery systems in backup powers and electric vehicles, a circulating electrolyte can be adopted to alleviate Al corrosion and hydrogen bubbling, such as by flushing out the hydrogen bubbles during battery operation and by emptying the channel during battery standby. As for portable electronics with low complexity tolerance, more fundamental corrosion inhibition techniques are requisite.

In literature, great efforts have been made to suppress the Al self-corrosion, which are mainly focused on Al alloying, electrolyte composition and cell structure innovations. For the Al anode, it was discovered that certain impurities such as Fe and Si can lead to significant Al corrosion [8]. Therefore, higher purity Al anode is desired despite its higher metal cost. On the contrary, other trace elements such as Zn, In, Mg, Ga and Sn inside the Al alloy were found to effectively suppress the Al corrosion [9–13]. In addition to Al alloying, the electrolyte composition can also be modified in order to suppress corrosion. Typically, strong alkaline solution such as KOH and NaOH is used as electrolyte, which can dissolve the protective Al_2O_3 layer on Al surface and corrode the Al inside. To alleviate this, different electrolyte additives were discovered, such as ZnO, Na_2SnO_3 , organic compounds and their mixture [14–18]. These additives can adsorb onto the Al surface either physically or chemically, protecting the fresh Al from severe corrosion. Alternatively, neutral electrolytes such as NaCl and sea water can be adopted to slow down Al corrosion, but with the price of decreased battery voltage and power [19]. Furthermore, innovative battery structures have been proposed to suppress corrosion. Chen et al. [20] designed a microfluidic Al-air battery with methanol-based anolyte and water-based catholyte. The low Reynolds number of the flow ensured a stable interface between the anolyte and catholyte, so that the Al corrosion in methanol anolyte was greatly inhibited. However, microfluidic fuel cells are very difficult to scale up that limits their applicability. To tackle this, Phusittananan et al. [21] and Teabnamang et al. [22] designed a new battery system with organic solution as anolyte and polymer gel as catholyte, which were separated by an anion exchange membrane. Either ethanol-ethylene glycol or methanol was adopted as the organic solvent, respectively. Moreover, Wang et al. [23] developed a more complex system using NaCl solution to separate the NaOH methanol solution (anolyte) and the HCl aqueous solution (catholyte). In general, the organic alkaline solution using alcohol as solvent is effective in suppressing the Al self-corrosion, but the bulky alcohol solution in battery may suffer from stability (evaporation) and safety (toxic) issues. Alternatively, Hopkins et al. [7] proposed an oil displacement method to protect the Al anode, in which a non-conducting oil could displace the alkaline electrolyte during battery standby, leading to a 99.99% reduction in corrosion. Nevertheless, all these novel systems require continuous pumping of the electrolyte, which is not practical for small-scale portable electronics.

Compared with liquid electrolytes either in static form or in continuous flow, the solid-state gel electrolytes are more

suitable for portable applications in terms of simplicity, energy density and safety, which can also be made flexible for powering wearable electronics [24–27]. Various polymers have been tried for the preparation of gel electrolytes, such as the polyvinyl alcohol (PVA) [24,28,29], polyacrylic acid (PAA) [25,30,31], sodium polyacrylate (PANa) [26], xanthan [32–34] and agarose [35]. Nevertheless, to date, most of the gel electrolytes in literature were developed based on water solvent, that is, the hydrogel electrolyte, which will trigger the Al corrosion reaction once the battery is assembled. In this manner, the Al anode and the other battery components need to be stored separately and assembled manually before usage, which is extremely inconvenient and creates safety issue. To tackle this, Zuo et al. [36] used an electrospun Al_2O_3 film to protect the Al anode from the corrosive gel electrolyte, which achieved a specific capacity of 1255 mA h g^{-1} at 5 mA cm^{-2} . Nevertheless, to further improve the anode stability and efficiency, an organic gel electrolyte with low cost and low toxicity would be more promising for Al-air batteries, such as the ethanol gel electrolyte, which has never been studied before to the best of our knowledge.

In this work, an ethanol gel electrolyte was proposed for Al-air battery, using polyethylene oxide (PEO) as the gelling agent and KOH as the alkaline source. The ethanol gel electrolyte was assembled in a portable Al-air battery with carbon paper as its air-breathing cathode and Al foil as anode. Before battery testing, Al stability inside the battery was confirmed at open circuit condition. Next, the power, impedance, discharge stability and energy efficiency was compared between the ethanol gel battery and the conventional water gel battery. Afterwards, the ethanol gel electrolyte was fully optimized by studying the effect of ethanol purity, polymer concentration and the gel thickness. Finally, a flexible version of the ethanol gel Al-air battery was developed by using paper as substrate, broadening its application prospect to flexible electronics.

2. Experimental

2.1. Ethanol gel preparation

Excess potassium hydroxide pellets (Fluka™) was dissolved in absolute ethanol solvent (BDH Chemicals) first to obtain the saturated KOH ethanol solution. According to Sigma-Aldrich and PubChem, 1 mass part of KOH can be dissolved in 3 mass parts of ethanol, leading to a concentration around 4.6 M. Next, 80 mg of polyethylene oxide (average molar mass of 2000,000, BOSF®) was stored in a cylindrical container (bottom area: 1.13 cm^2), and 200 μL of the KOH-ethanol solution was added into the PEO powder dropwise. Afterwards, the container was stored overnight to allow the slow gelling process, which should also be sealed to avoid ethanol evaporation and water vapor uptake.

The as-prepared ethanol gel is a flexible, elastic and viscous solid, which should be sealed for storage in order to avoid the continuous evaporation loss of ethanol solvent. Fig. 1a characterizes the gel micro morphology by a Scanning Electron Microscope (Hitachi S3400N) with attached Energy

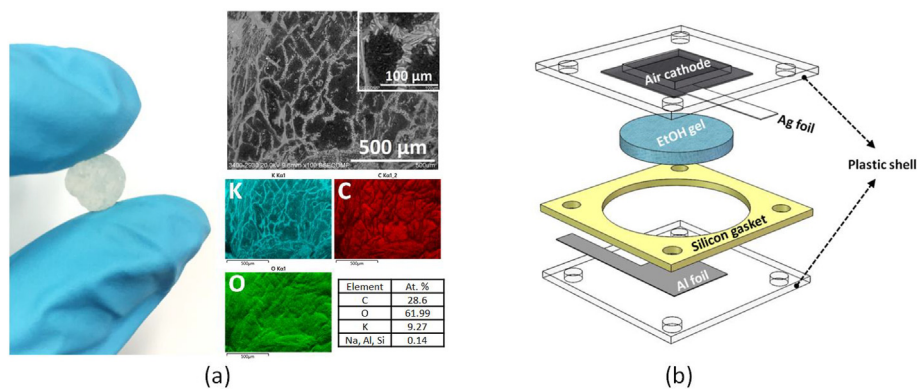


Fig. 1. Design of the Al-air battery with ethanol gel electrolyte: (a) Digital image, SEM image and element composition of the ethanol gel electrolyte; (b) Exploded view of the battery structure.

Dispersive X-ray Detector. A bright network consisting of micro crystals was observed on the gel surface, which should be the precipitated KOH due to the highly vacuum environment inside SEM that accelerated ethanol evaporation. The element mapping proves this speculation, as the K element from KOH was mainly located in the network area, while the C element from PEO and remaining ethanol existed in the bulk area. As for the O element, it was uniformly distributed on the gel surface, which came from KOH, PEO and ethanol.

2.2. Battery design

The solid-state Al-air battery has a similar structure with our previous work except for the electrolyte part [37]. As shown in Fig. 1b, the Al foil anode and the air cathode were attached to plastic shells made of 2 mm-thick polymethyl methacrylate (PMMA). Both the Al foil area and the cathode window area were 1 cm × 1 cm, which was used for current/power density calculation. The ethanol gel electrolyte was placed between the two PMMA layers, while a 1 mm-thick silicon gasket was also added to avoid water vapor uptake and control gel thickness at the same time. Finally, the battery was assembled by bolts and nuts in the periphery, and the cathode window was sealed by tape before testing.

Both high purity (99.999% and 99.9%, aladdin®) and low purity (98.2%, kitchen foil) Al foils were used as anode, while blank carbon paper, MnO₂-coated carbon paper (1.2 mg cm⁻² MnO₂) and Pt-coated carbon paper (1.2 mg cm⁻² Pt) were used as cathode. After consumption, the Al anode and ethanol gel electrolyte could be replaced manually to achieve battery mechanical rechargeability.

2.3. Battery test and characterization

Before battery testing, the cathode sealing tape was removed to allow air diffusion. The battery open circuit voltage (OCV) was recorded first. Next, the polarization curve was obtained by linear sweep voltammetry (LSV) from OCV to 0 V with a scan rate of 10 mV s⁻¹. To obtain the ohmic resistance, electrochemical impedance spectroscopy (EIS) test

was conducted at OCV from 100 k Hz to 0.1 Hz, with an amplitude of 10 mV. To investigate the discharge lifetime and the specific capacity of Al anode, long-term Galvanostatic discharge was also conducted at 0.1–1 mA cm⁻², and the Al anode weight before and after discharge was recorded. To remove the Al(OH)₃ product on the anode surface, the used Al foil was polished by sandpaper and sonicated, which was also fully dried before weighing. In addition, the used Al foil without product removal was characterized by SEM to investigate the variation of surface morphology.

For comparison purpose, an Al-air battery with a conventional water gel electrolyte was also tested in the same way. The water gel was prepared by using 1 M KOH instead of KOH-ethanol solution, and sodium polyacrylate (average molar mass of 5000,000–7000,000, Macklin®) instead of PEO. All the other parameters were kept the same for comparison.

3. Results & discussion

3.1. Al corrosion comparison

Before studying the performance of the battery, the corrosion rate of Al foil in both a KOH water solution (1 M) and a KOH ethanol solution (saturated) was compared. As shown in Fig. 2a, the Al foil in KOH water solution would disappear completely within a few hours due to vigorous corrosion, while it could be kept in KOH ethanol solution for more than 30 days with a total weight loss of only 3.4%. The weight loss was due to the mild corrosion in the beginning because the “pure” ethanol still contained trace amount of water inside (Video S1 in supplementary material). Also, the strong alkaline would react mildly with ethanol to generate water as well. Here, it is worth mentioning that the KOH ethanol solution would gradually turn brown, which is probably due to the partial oxidation of ethanol in strong alkaline and the impurities associated with the KOH pellet. Nevertheless, this variation was found to have negligible effect on the battery performance. Fig. 2b and c compares the surface morphology of Al anode after immersed in KOH ethanol solution or KOH

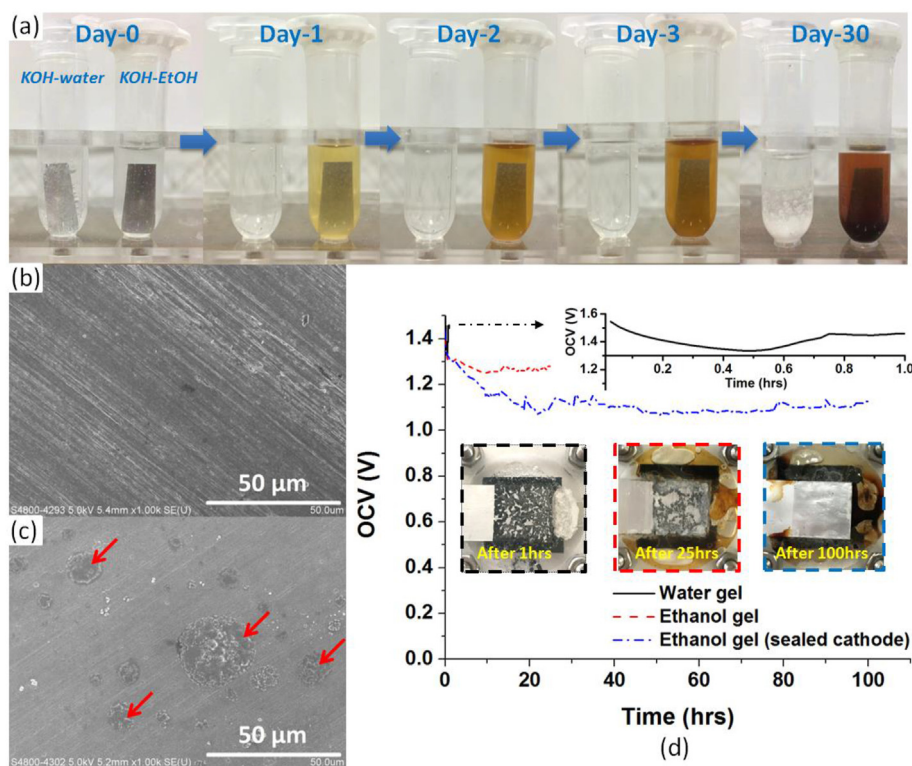


Fig. 2. Comparison of Al corrosion in different solvent: (a) Corrosion test in KOH water solution and KOH ethanol solution; (b) Surface morphology of the Al foil after immersed in KOH ethanol solution; (c) Surface morphology of the Al foil after immersed in KOH water solution; (d) OCV test of the Al-air battery with water gel electrolyte or ethanol gel electrolyte.

water solution for several minutes. For the former case, the variation of Al surface was negligible when compared with the pristine Al foil (Fig. S1 in supplementary material). As for the latter case, distinct corrosion products were observed on the Al surface (red arrows), indicating a fast corrosion reaction. Furthermore, to prove the stability of Al anode inside the battery, OCV of the assembled Al-air battery was recorded, using either the water gel or the ethanol gel. As shown in Fig. 2d, the water gel-based battery only lasted for 1 h (upper inset) before the Al foil completely disappeared due to corrosion, while the ethanol gel-based battery could last for 25 h before the Al foil fully corroded. Here, the Al foil in ethanol gel-based battery would also be corroded because the ethanol gel can absorb water vapor from ambient continuously via the air-breathing cathode. To avoid this issue, the air-breathing cathode was sealed when the battery was not at work, leading to an intact Al anode even after 100 h' OCV test (Fig. 2d).

3.2. Electrode selection

Different types of oxygen reduction catalysts and different purities of Al foils were examined in this section, in order to select the most suitable electrode materials for the ethanol gel Al-air battery. For the cathode side, both Pt and MnO_2 are common catalyst for the oxygen reduction reaction (ORR). As shown in Fig. 3a, when Pt/C was used as cathode catalyst, the OCV was only 1.1 V, which was much lower than MnO_2/C

and even the blank carbon paper. This is due to the fact that Pt is a fine catalyst for ethanol oxidation (from the ethanol gel) and induces mixed potential on the cathode side, which is similar to the fuel crossover effect in direct ethanol fuel cells. Therefore, Pt was not suitable for the ethanol gel Al-air battery. On the contrary, MnO_2 is not active towards ethanol oxidation, which output a normal OCV of 1.4 V similar to the blank carbon paper. Also, its power output was 65% higher than blank carbon paper. To further determine the suitable cathode catalyst, the discharge behavior of the battery at both 0.1 and 1.0 mA cm^{-2} were compared in Fig. S2 (supplementary material). It was observed that the difference among blank carbon paper, MnO_2 and Pt was not significant at this current density range. Therefore, blank carbon paper was selected for further study considering its lowest cost and environmental benignity.

The purity of Al was also reported to have significant effect on Al-air battery performance [38]. As shown in Fig. 3b, the OCVs of 99.9% and 99.999% pure Al were 0.3 V higher than that of kitchen foil Al (98.2% purity), and the battery voltage was also higher at other discharge current densities. The peak power densities were 2.6, 4.0 and 3.2 mW cm^{-2} for the kitchen foil Al, 99.9% Al and 99.999% Al, respectively. By EDX analysis, it was found that the kitchen foil Al contained about 0.33% Fe and 0.39% Si impurities while the 99.9% and 99.999% Al did not, which were reported to be the cathodic impurities that caused the shift of anode potential towards the noble direction. In addition, the present of Fe impurity would

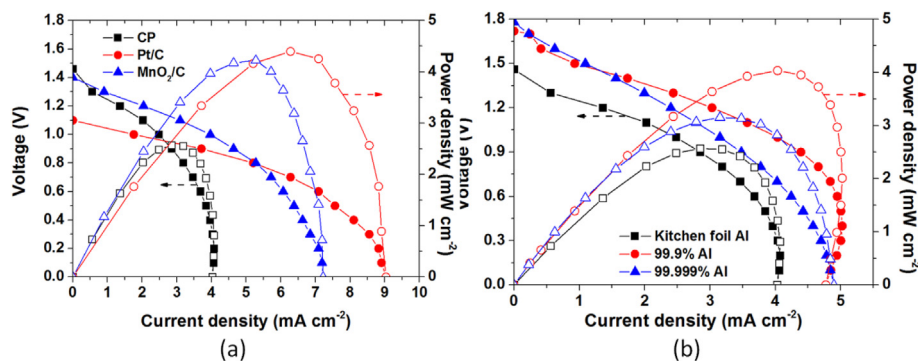


Fig. 3. Comparison of the ethanol gel Al-air battery performance using different electrode materials: (a) Effect of ORR catalyst species (with kitchen foil Al as anode); (b) Effect of Al purity (with blank carbon paper as cathode).

lead to severer Al self-corrosion, which is detrimental to the discharge efficiency [8]. As for the inferior performance of the 99.999% Al, it could be related to the more stable passive film on its surface, which restricted the electrochemical active area compared with the less pure 99.9% Al, especially at the high current density range [38]. As a consequence, 99.9% Al was the most suitable anode material in terms of both performance and cost.

3.3. Battery performance comparison

This section compares the Al-air battery performance between the ethanol gel electrolyte and the water gel electrolyte. As shown in Fig. 4a, both the water gel battery and the ethanol gel battery obtained high OCV near 1.8 V, but the current and

power densities were much higher for the water gel battery, which reached 19.7 mA cm^{-2} and 15.9 mW cm^{-2} , respectively. On the contrary, the ethanol gel battery only achieved 5.0 mA cm^{-2} and 4.0 mW cm^{-2} . From the slope of middle part of the polarization curves (0.9–1.5 V), it can be inferred that this performance difference is mainly due to the much higher ionic resistance of the ethanol gel than the water gel. In addition, it was observed that both the two batteries encountered significant mass transport resistance at the low voltage region (below 0.9 V), which could be due to the insufficient OH^- supply to the Al oxidation reaction at anode (Eq. (1)). Fig. 4b confirms the above speculation, in which the battery ohmic resistance was 1.4 and $34.1 \text{ } \Omega$ for the water gel and ethanol gel electrolytes, respectively. Also, the polarization resistance of ethanol gel battery was much higher as can be

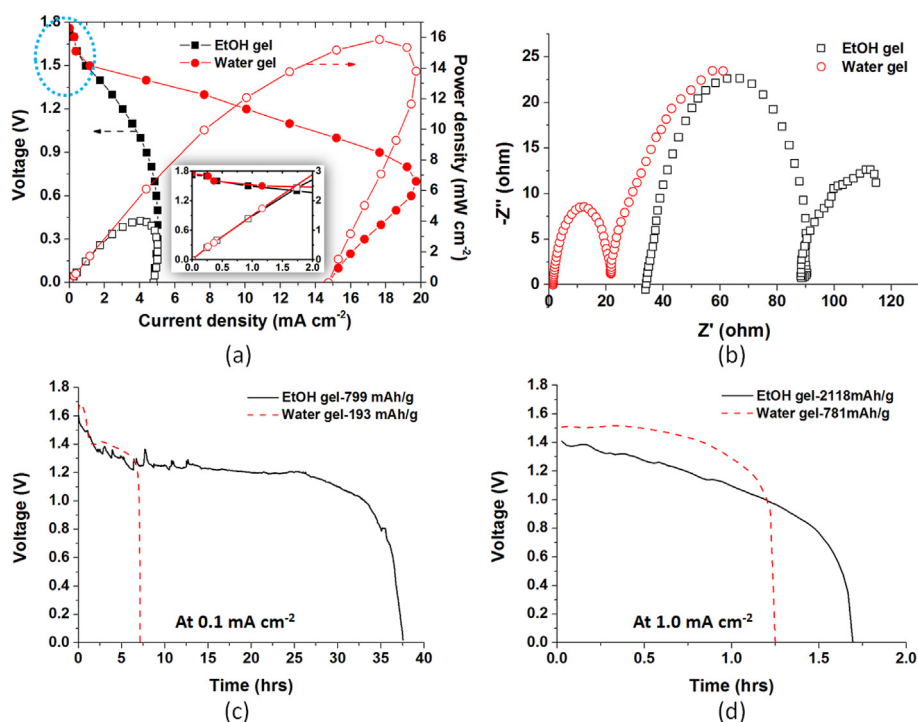
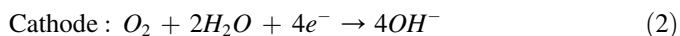
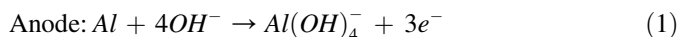


Fig. 4. Comparison of battery performance between water gel and ethanol gel: (a) Polarization curves; (b) EIS curves at OCV (c–d) Galvanostatic discharge at 0.1 and 1.0 mA cm^{-2} .

seen from the larger arc radius at the high frequency range, which could be attributed to the insufficient water supply to the ORR at cathode (Eq. (2)).



In literature, conventional Al-air batteries with flowing aqueous electrolyte can achieve peak power density of hundreds of mW cm^{-2} , which is mainly benefited from the sufficient OH^- supply as well as the high diffusivity inside aqueous solvent [7]. On the contrary, solid-state Al-air batteries with gel electrolyte generally achieve a few or tens of mW cm^{-2} due to the impeded ionic diffusion inside the polymer gel [31,39,40]. As for the present ethanol gel Al-air battery, the ionic resistance was further increased as can be seen in the battery EIS test. From literature, the electric conductivity of water-based solution is much higher than ethanol-based solution, which is mainly attributed to the higher permittivity of water than ethanol [41]. For instance, the conductivity of potassium acetate water solution is 50–100 times higher than that of potassium acetate ethanol solution at different solute concentrations. Therefore, the present ethanol gel Al-air battery exhibited a lower power output, and the working voltage dropped evidently when discharge current increased. To further improve its electrochemical performance, alternatively organic solvent with higher permittivity is desired, which should also allow high-concentration KOH dissolution. In the meantime, low volatility and low hygroscopicity are also important properties to avoid solvent evaporation and water vapor uptake in the ambient environment.

Despite the lower power and current output, the ethanol gel battery exhibited a promising performance at the low current region (below 2 mA cm^{-2}), which was similar to the water gel battery (inset of Fig. 4a). In the meantime, the Al corrosion can be significantly inhibited. As shown in Fig. 4c, when discharged at 0.1 mA cm^{-2} , the ethanol gel battery could last for 37.6 h, which was 5.3 times of the water gel cell. In addition, the specific capacity reached 799 mA h g^{-1} , which was 4.1 times of the water gel cell. This indicates that the ethanol gel electrolyte enables much less Al self-corrosion during the long-term discharge. Fig. 4d compares the battery discharge at 1 mA cm^{-2} . At a higher current, the Al oxidation reaction competes better with the Al corrosion reaction, leading to a higher discharge specific capacity. This time, the ethanol gel battery achieved a high specific capacity of 2118 mA h g^{-1} , which was 71.1% of the theoretical value (2980 mA h g^{-1}) and 2.7 times of the water gel case. In summary, the ethanol gel Al-air battery is more suitable for low current density applications with much less Al self-corrosion.

Table 1 compares the performance of Al-air batteries using solid-state gel electrolyte in literature. For those batteries using hydrogels, the peak power density ranges from 1.2 to 91.1 mW cm^{-2} , which is significantly determined by the ionic conductivity of different gel compositions. The specific capacities achieved are generally much lower than the theoretical

value due to Al corrosion, despite the high purity Al and electrolyte corrosion inhibitors used. As for the present ethanol gel Al-air battery, the peak power density is moderate, but the specific capacity of 2118 mA h g^{-1} is among the highest, which can be further improved to 2546 mA h g^{-1} via gel property optimization, as will be discussed in the following section.

After discharge, the used Al foil was detached from the battery and rinsed completely to remove any gel residue on its surface. Fig. 5 compares the surface morphology of Al foils from the water gel battery and the ethanol gel battery. Apparently, the former case exhibited a much rougher surface than the latter, from both the SEM and digital images in Fig. 5a and b. With a higher magnification, it was observed that the Al foil in water gel had non-uniform protuberances and cracks on its surface (Fig. 5c), which should be the $\text{Al}(\text{OH})_3$ product from both Al oxidation and Al corrosion reactions. As for the Al foil in ethanol gel, two different morphologies were found on its surface, one with ripple shape occupied most of the surface while the other with stripe shape distributed separately on the surface (Fig. 5d). The ripple shape area should be related to Al oxidation reaction while the stripe shape islands should be related to Al corrosion. To prove this hypothesis, another ethanol gel Al-air battery was discharged in a dry room (plastic box with excessive silica gel desiccant) to avoid any water vapor uptake, and the used Al foil was examined by SEM (Fig. S3 in supplementary material). This time, only the ripple area was found on its surface. From the above discussion, it can be concluded that the ethanol gel electrolyte can indeed suppress Al self-corrosion, but the continuous water vapor uptake from ambient still triggers a certain extent of corrosion. To avoid this, alternative organic solvent that has no hygroscopicity could be a better choice than ethanol, which will be explored in our future research.

3.4. Parametric study on gel properties

3.4.1. Effect of ethanol purity

The battery performance with ethanol gel electrolyte is significantly restricted by its high ionic resistance, which can be improved by using less pure ethanol solvent. In this section, 100, 95 and 90 vol.% pure ethanol was used for KOH solution preparation, which was next used to fabricate the ethanol gel. As shown in Fig. 6a, the battery performance was gradually improved as the water content in gel increased. The OCV was all around 1.8 V, while the peak power density and maximum current density increased from 4.0 to 7.1 mW cm^{-2} and from 5.0 to 10.2 mA cm^{-2} , respectively. Fig. 6b compares the impedance of the battery with the three ethanol purities. Indeed, their ohmic resistance decreased from 34.1 to 21.0Ω , while the polarization resistance was also gradually decreased, which would be the major reason behind the performance improvement.

Nevertheless, the introduction of water content inevitably increases Al self-corrosion. Fig. 6c and d compares the discharge lifetime of the three ethanol purities at 0.1 and

Table 1
Performance comparison among Al-air batteries with gel electrolyte in literature.

Reference	Al anode	Gel electrolyte	Air cathode	OCV	Peak power density	Specific capacity
Wu et al. [39]	99.99% Al plate	KOH + PVA/PAA	KMnO ₄ /C	1.5 V ^a	1.2 mWcm ⁻²	
Mohamad et al. [40]	95.28% Al plate	KOH + hydroponics gel	MnO _x /C	1.94 V	5.5 mWcm ⁻²	105 mAhg ⁻¹
Zhang et al. [31]	Al mesh	KOH + ZnO + PAA	La ₂ O ₃ + SrO + MnO ₂	1.3–1.35 V ^a	91.1 mWcm ⁻²	1166 mAhg ⁻¹
Pino et al. [30]	Commercial Al alloys	KOH + ZnO + PAA	MnO ₂ /C			426 mAhg ⁻¹
Xu et al. [24]	99.999% Al spring	KOH + ZnO + Na ₂ SnO ₃ + PVA + PEO	Ag/CNT	1.7 V	^a 1.5 mWcm ⁻²	935 mAhg ⁻¹
Di Palma et al. [32]	99.998% Al foil	k-carrageenan + KOH	Pt/C	1.7 V		400 mAhg ⁻¹
Shen et al. [29]	Al plate	KOH + PVA	Co–N/CNs	1.4 V ^a	41.5 mWcm ⁻²	
Ma et al. [25]	Al foil	KOH + ZnO + Na ₂ SnO ₃ + In(OH) ₃ + PAA	Fe ₃ C@N-CFs	1.8 V ^a	41.5 mWcm ⁻²	1287.3 mAhg ⁻¹
Sun et al. [35]	99.99% Al foil	NaOH + ZnO + Na ₂ SnO ₃ + agarose gel	N-doped graphene	1.4 V ^a	26.9 mWcm ⁻²	2148.5 mAhg ⁻¹
Present work	99.9% Al foil	KOH + EtOH + PEO	Carbon paper	1.72 V	4 mWcm ⁻²	2118 mAhg ⁻¹ (2546 mAhg ⁻¹)

^a Estimated from the figure.

1.0 mA cm⁻², respectively. The discharge curves did not varied significantly, but the calculated specific capacity was quite different. In general, there was a reduction trend of specific capacity when the water content in the gel electrolyte increased. In fact, this reduction was more distinct when compared with pure water gel in Fig. 4c and d. Therefore, it is concluded that the pure ethanol gel is more favored for low current operation in terms of storage stability and discharge efficiency. However, when higher power output is demanded, a less pure ethanol gel can be used instead.

3.4.2. Effect of polymer concentration

The polymer concentration in the gel electrolyte directly determines its ionic conductivity, which should achieve a fine balance between the solidification degree and the ion diffusivity inside. As shown in Fig. 7a, when the PEO concentration increased from 200 to 600 mg mL⁻¹, the peak power density gradually decreased from 4.4 to 2.6 mW cm⁻², and the maximum current density decreased from 6.4 to 3.4 mA cm⁻². From the inset, it was observed that the gel electrolyte with 600 mg mL⁻¹ PEO suffered from incomplete gelling, leaving white PEO powder inside the gel. As for the gel electrolyte with 200 mg mL⁻¹ PEO, it suffered from insufficient solidification, which could easily tear apart during transportation. Therefore, 400 mg mL⁻¹ was regarded as a proper concentration. Fig. 7b shows that the 200 mg mL⁻¹ case obtained the lowest ohmic resistance of 20 Ω, while the 600 mg mL⁻¹ case obtained the highest value of 40.4 Ω. The polarization resistance also rose as the PEO concentration increased, which was mainly due to the more and more difficult supply of OH⁻ to the anode surface.

Fig. 7c and d show the effect of polymer concentration on the battery discharge lifetime and specific capacity. When the polymer concentration increased, the discharge lifetime decreased at both 0.1 and 1.0 mA cm⁻², which was mainly due to the impeded OH⁻ transport inside the gel. Since the gelling skeleton was made of crosslinked polymer chains, the 600 mg mL⁻¹ case with more concentrated polymer chains

would exhibit stronger resistance to the diffusion of OH⁻ inside. In this manner, the anode Al oxidation will be forced to stop earlier due to the insufficient OH⁻ supply. On the other hand, the discharge specific capacity was improved with a higher polymer concentration of 600 mg mL⁻¹. This was probably related to the transport of the absorbed water from cathode to anode inside the gel, which can intensify the Al corrosion once it diffused to the Al surface. As a consequence, the 600 mg mL⁻¹ case achieved the lowest water transport rate and Al self-corrosion, leading to the highest discharge efficiency. In summary, a moderate polymer concentration of 400 mg mL⁻¹ is more favorable, which can achieve a fine balance among mechanical strength, power output, discharge lifetime and specific capacity.

3.4.3. Effect of gel thickness

The gel thickness not only determines the ionic conductivity but also affects the delivery of hydroxyl ions and water inside. In this section, different thicknesses of the silicon gasket (0.5, 1 and 2 mm) were used to control the gel thickness, while the total amount of gel electrolyte was kept identical. As shown in Fig. 8a, with the increase of gel thickness, the battery performance dropped significantly. The peak power density decreased from 5.8 to 2.7 mW cm⁻², while the maximum current density decreased from 7.4 to 3.6 mA cm⁻², when the gel thickness increased from 0.5 to 2 mm. Fig. 8b reveals the much lower ohmic resistance of 14.5 Ω for the 0.5 mm thick gel, compared with 76 Ω for the 2.0 mm thick gel. Also, the polarization resistance was much lower for the thinner gel.

Fig. 8c and d illustrates the battery discharge lifetime at 0.1 and 1.0 mA cm⁻², respectively. It is evident that the 0.5 mm thick gel achieved much shorter discharge than thicker gels, together with the lowest specific capacity. On the contrary, the 2 mm thick gel exhibited the longest discharge and highest specific capacity, which even reached 2546 mA h g⁻¹ at 1.0 mA cm⁻² (85.4% of theoretical value). This phenomenon can be explained by the schematic

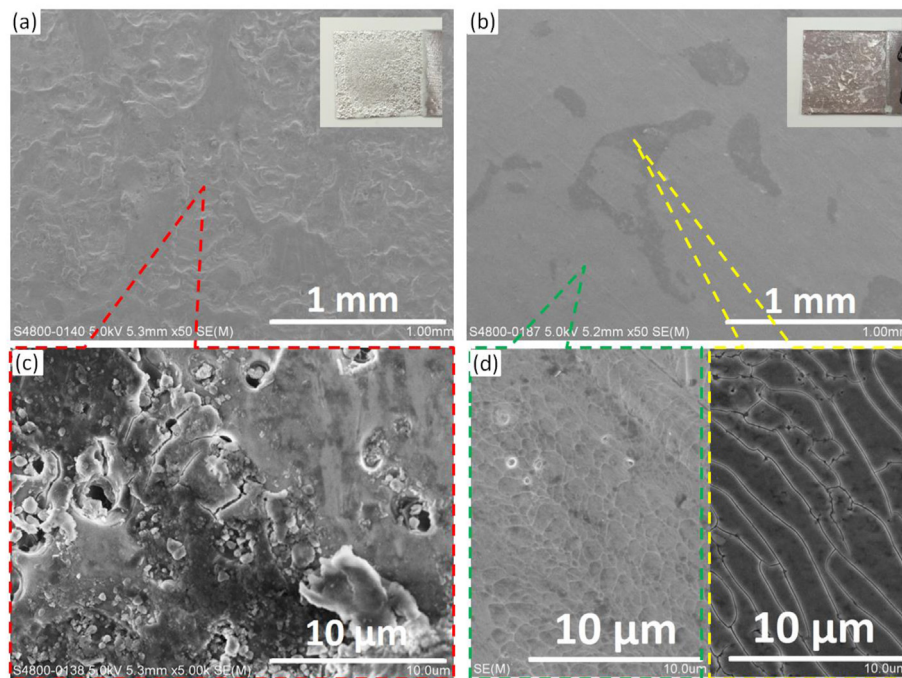


Fig. 5. Surface morphology of the Al foil anode after long-term discharge: (a) with water gel electrolyte (low-magnification, inset: digital image); (b) with ethanol gel electrolyte (low-magnification, inset: digital image); (c) with water gel electrolyte (high-magnification); (d) with ethanol gel electrolyte (high-magnification).

diagram of OH^- diffusion in the inset of Fig. 8c. For the thinner gel, the OH^- reserve in its periphery was far away from the electrode area, so it took a longer diffusion path before it could participate in the anode reaction. On the contrary, the OH^- reserve in the top area of the thicker gel was much easier to reach the anode surface, which better

supported the long-term discharge. As for the discharge efficiency, the shorter electrode distance with a thinner gel allows more efficient water transport from cathode to anode, leading to severer Al self-corrosion. In summary, a moderate gel thickness is favored for the present ethanol gel Al-air battery in terms of power and efficiency.

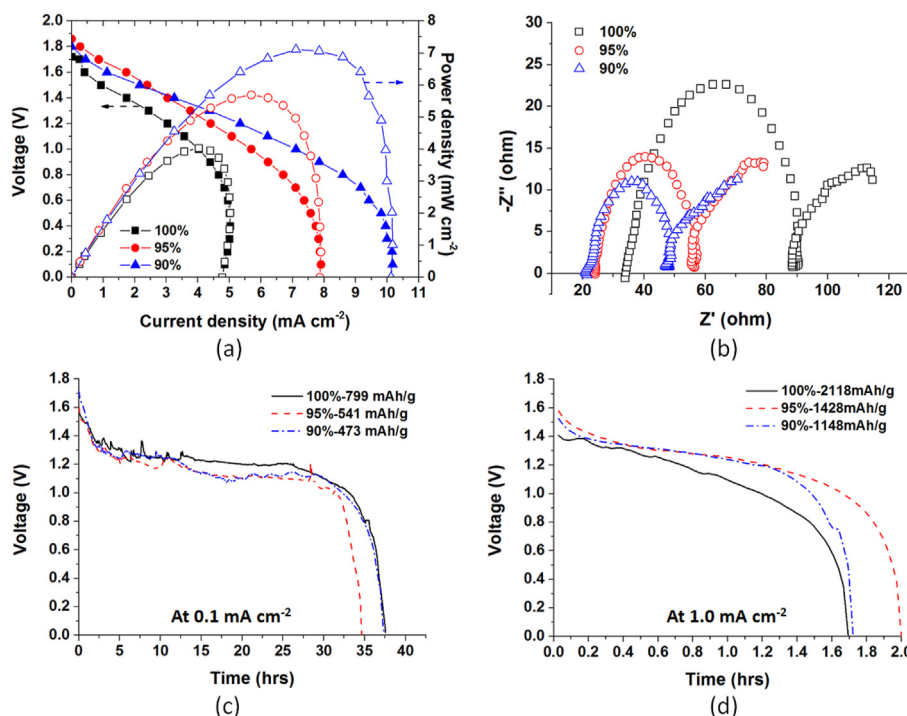


Fig. 6. Effect of ethanol purity on the battery performance: (a) Polarization curves; (b) EIS curves at OCV (c–d) Galvanostatic discharge at 0.1 and 1.0 mA cm^{-2} .

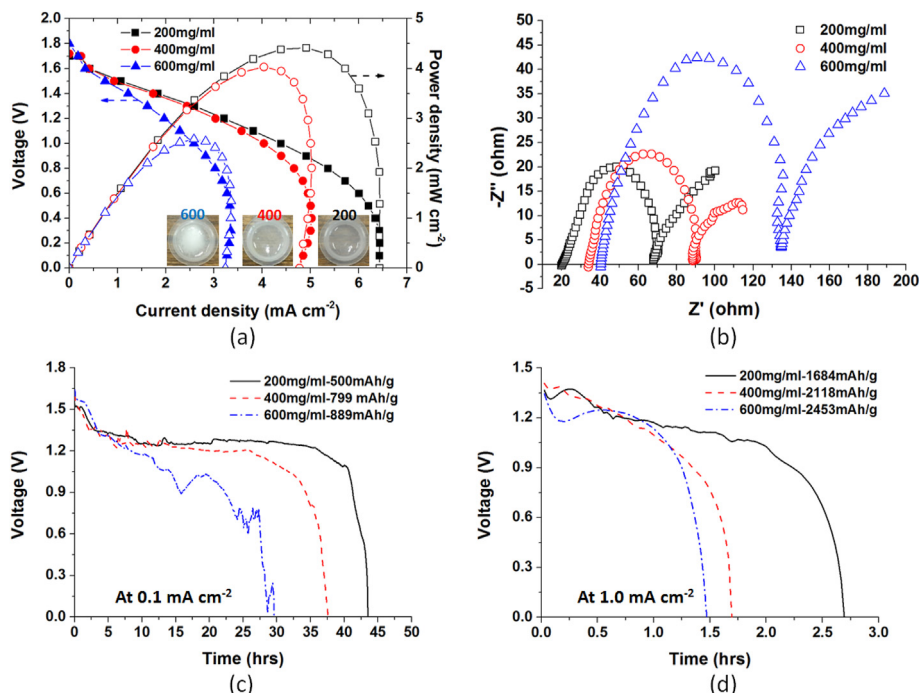


Fig. 7. Effect of polymer concentration on the battery performance: (a) Polarization curves (inset: image of the different gel electrolytes); (b) EIS curves at OCV (c-d) Galvanostatic discharge at 0.1 and 1.0 mA cm⁻².

3.5. Flexible battery design

The ethanol gel electrolyte can also be impregnated into a paper substrate in order to obtain a flexible paper-based Al-air battery. Fig. 9a shows the fabrication process of the battery prototype. First, a commercial carbon paste (Jelcon CH-8) was printed onto a filter paper (Whatman®, 0.2 mm thickness) using a

home-made 3D printer [42], which had a grid pattern (1 cm² total area) in order to support the cathode ink [43]. Next, a commercial N-CNT ink (Aladdin®) was deposited within the carbon grid as the air-breathing cathode, with a total N-CNT loading of 1 mg cm⁻². Afterwards, 100 μL of a thin ethanol gel (30 mg mL⁻¹ PEO in pure ethanol) was dropped onto the back-side of the filter paper, with an annular plastic chip fixing its edges

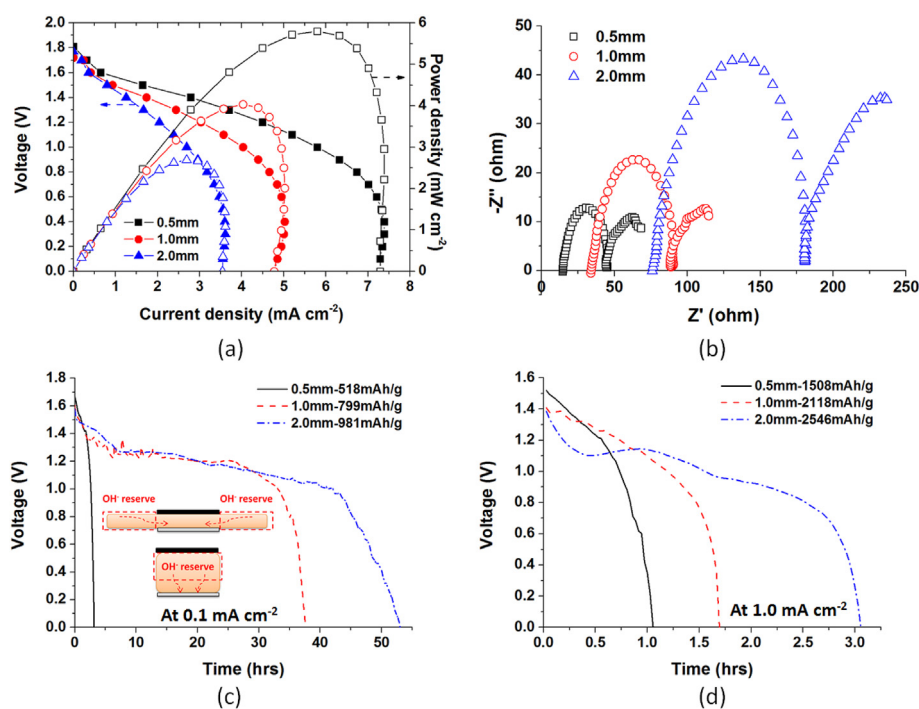


Fig. 8. Effect of gel thickness on the battery performance: (a) Polarization curves; (b) EIS curves at OCV; (c) Galvanostatic discharge at 0.1 mA cm⁻² (inset: schematic diagram of hydroxyl transport); (d) Galvanostatic discharge at 1.0 mA cm⁻².

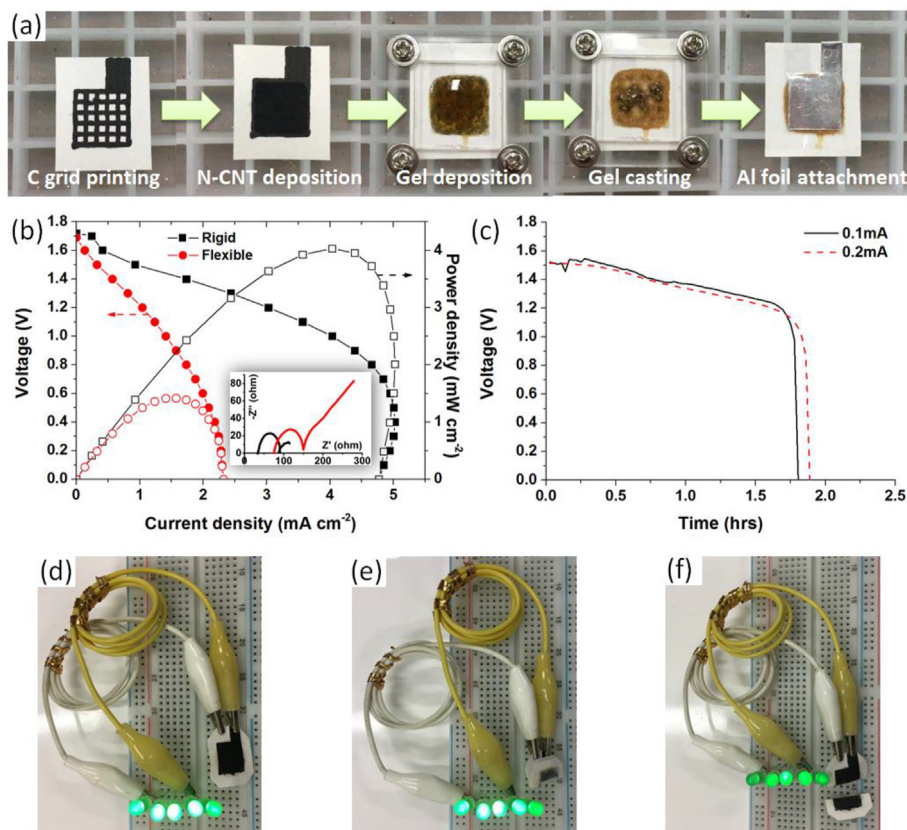


Fig. 9. A flexible Al-air battery with ethanol gel electrolyte: (a) Fabrication process; (b) Performance comparison between the rigid cell and the flexible cell (inset: EIS curves at OCV); (c) Discharge curves at 0.1 and 0.2 mA cm⁻² (d-f) Demonstration of a 2-cell battery pack powering LED lights when it was intact, bended and cut into half, respectively.

in order to avoid paper shrinkage in contact with strong alkaline. Here, the thin ethanol gel was used so that it could maintain a semi-fluid property and be absorbed easily into the cellulose network. After casting at 60 °C for 5 min, the excess ethanol solvent was removed, and a concentrated ethanol gel electrolyte inside the paper was obtained, whose thickness was determined by the paper thickness. Lastly, an Al foil anode was fixed onto the paper by taping, and the obtained flexible Al-air battery was sealed for storage. During the fabrication process, no metal materials were used except for the Al anode, which was very friendly to the environment.

Fig. 9b compares the performance between this flexible battery design and the previous rigid battery design. Apparently, the flexible battery suffered from lower power output, with a peak power density of only 1.4 mW cm⁻². This was mainly due to its less conductivity, which was more than two times of the rigid battery as indicated by the EIS curves in the inset. This insufficient conductivity was derived from both the high-resistance carbon grid for supporting the cathode, and the porous paper substrate for supporting the gel electrolyte, which sacrificed battery power in exchange for device flexibility and cost effectiveness. In addition, Fig. 9c shows the battery discharge at 0.1 and 0.2 mA cm⁻², in which both cases obtained a discharge lifetime of 1.8–1.9 h. This short discharge lifetime was attributed to the limited gel storage capacity inside a thin paper, which could be increased by using

thicker paper substrates with higher porosity. Furthermore, Fig. 9d–f demonstrates a flexible Al-air battery pack (2 cells in series) for LED lighting at different status. Benefited from the flexible and mild materials, the current battery could function normally even bended by 180° or cut into half, proving its high flexibility and safety level during practical applications.

4. Conclusion

In this work, an ethanol gel electrolyte was developed for Al-air batteries for the first time. KOH was dissolved in pure ethanol to form a saturated solution first, which was next solidified by PEO to form a flexible and stretchable gel electrolyte. When assembled in a micro Al-air battery with Al foil anode and carbon paper cathode, a peak power density of 4 mW cm⁻² was obtained, which was lower than the battery with water gel electrolyte due to the higher ionic resistance. Nevertheless, their discharge performances at low current densities (less than 2 mA cm⁻²) were quite similar with each other. More importantly, the Al-air battery with ethanol gel electrolyte achieved much longer discharge lifetime and higher energy efficiency than the one using water gel electrolyte, proving that Al corrosion was significantly inhibited. By studying various parameters of the ethanol gel, it was found that the battery performance could be improved by adding 5–10% water into the ethanol solvent, but the discharge efficiency would be sacrificed to some extent. Also, a lower polymer concentration

and a smaller gel thickness could improve the battery power output, but both at a cost of reduced discharge efficiency due to the easier water transport from cathode to anode. Therefore, a moderate polymer concentration and gel thickness were desired to balance the battery power and efficiency. Finally, to cater the need of flexible electronics, a paper-based Al-air battery was developed by impregnating the ethanol gel electrolyte into a paper substrate, which could function normally even under deformation or serious damage.

Declaration of competing interest

The authors declare that they have no known competing financial interests or personal relationships that could have appeared to influence the work reported in this paper.

Acknowledgement

The authors would like to acknowledge the SZSTI of Shenzhen Municipal Government (JCYJ20170818141758464) and the CRCG grant of the University of Hong Kong (201910160008) for providing funding support to the project.

Appendix A Supplementary data

Supplementary data to this article can be found online at <https://doi.org/10.1016/j.gee.2021.05.011>.

References

- [1] M.A. Rahman, X. Wang, C. Wen, *J. Electrochem. Soc.* 160 (2013) A1759.
- [2] P. Goel, D. Dobhal, R. Sharma, *Journal of Energy Storage* 28 (2020) 101287.
- [3] Y. Wang, H. Kwok, W. Pan, H. Zhang, D.Y. Leung, *J. Power Sources* 414 (2019) 278–282.
- [4] X. Ou, G. Zhang, S. Zhang, X. Tong, Y. Tang, *Energy Storage Materials* 28 (2020) 357–363.
- [5] H. Wang, Y. Tang, *Chem. Res. Chin. Univ.* 36 (2020) 402–409.
- [6] M. Wang, Q. Liu, G. Wu, J. Ma, Y. Tang, *Green Energy Environ.* (2021).
- [7] B.J. Hopkins, Y. Shao-Horn, D.P. Hart, *Science* 362 (2018) 658–661.
- [8] Y.-J. Cho, I.-J. Park, H.-J. Lee, J.-G. Kim, *J. Power Sources* 277 (2015) 370–378.
- [9] M. Jingling, R. Fengzhang, W. Guangxin, X. Yi, L. Yaqiong, W. Jiuba, *Int. J. Hydrogen Energy* 42 (2017) 11654–11661.
- [10] R. Liang, Y. Su, X.-L. Sui, D.-M. Gu, G.-S. Huang, Z.-B. Wang, *J. Solid State Electrochem.* 23 (2019) 53–62.
- [11] I.-J. Park, S.-R. Choi, J.-G. Kim, *J. Power Sources* 357 (2017) 47–55.
- [12] Z. Sun, H. Lu, *J. Electrochem. Soc.* 162 (2015) A1617.
- [13] Z. Wu, H. Zhang, C. Guo, J. Zou, K. Qin, C. Ban, H. Nagaumi, *J. Solid State Electrochem.* 23 (2019) 2483–2491.
- [14] H. Jiang, S. Yu, W. Li, Y. Yang, L. Yang, Z. Zhang, *J. Power Sources* 448 (2020) 227460.
- [15] X. Li, J. Li, D. Zhang, L. Gao, J. Qu, T. Lin, *J. Mol. Liq.* 322 (2021) 114946.
- [16] O. Taeri, A. Hassanzadeh, F. Ravari, *ChemElectroChem* 7 (2020) 2123–2135.
- [17] S. Wu, Q. Zhang, D. Sun, J. Luan, H. Shi, S. Hu, Y. Tang, H. Wang, *Chem. Eng. J.* 383 (2020) 123162.
- [18] L. Yang, Y. Wu, S. Chen, Y. Xiao, S. Chen, P. Zheng, J. Wang, J.-E. Qu, *Mater. Chem. Phys.* 257 (2021) 123787.
- [19] Y. Wang, H.Y. Kwok, W. Pan, Y. Zhang, H. Zhang, X. Lu, D.Y. Leung, *Electrochim. Acta* 319 (2019) 947–957.
- [20] B. Chen, D.Y. Leung, J. Xuan, H. Wang, *J. Power Sources* 336 (2016) 19–26.
- [21] T. Phusittananan, W. Kao-Ian, M.T. Nguyen, T. Yonezawa, R. Pornprasertsuk, A.A. Mohamad, S. Kheawhom, *Frontiers in Energy Research* 8 (2020) 189.
- [22] P. Teabnamang, W. Kao-Ian, M.T. Nguyen, T. Yonezawa, R. Cheacharoen, S. Kheawhom, *Energies* 13 (2020) 2275.
- [23] L. Wang, R. Cheng, C. Liu, M. Ma, W. Wang, G. Yang, M. Leung, F. Liu, S. Feng, *Materials Today Physics* 14 (2020) 100242.
- [24] Y. Xu, Y. Zhao, J. Ren, Y. Zhang, H. Peng, *Angew. Chem.* 128 (2016) 8111–8114.
- [25] Y. Ma, A. Sumbaja, W. Zang, S. Yin, S. Wang, S.J. Pennycook, Z. Kou, Z. Liu, X. Li, J. Wang, *ACS Appl. Mater. Interfaces* 11 (2018) 1988–1995.
- [26] Y. Wang, W. Pan, H.Y. Kwok, H. Zhang, X. Lu, D.Y. Leung, *J. Power Sources* 437 (2019) 226896.
- [27] Y. Yu, Y. Zuo, Y. Liu, Y. Wu, Z. Zhang, Q. Cao, C. Zuo, *Nanomaterials* 10 (2020) 216.
- [28] M. Gaele, F. Migliardini, T. Di Palma, *J. Solid State Electrochem.* (2021) 1–10.
- [29] J. Shen, L. Meng, Y. Liu, C. Chen, Y. Zhu, C. Li, *RSC Adv.* 8 (2018) 22193–22198.
- [30] M. Pino, J. Chacón, E. Fatás, P. Ocón, *J. Power Sources* 299 (2015) 195–201.
- [31] Z. Zhang, C. Zuo, Z. Liu, Y. Yu, Y. Zuo, Y. Song, *J. Power Sources* 251 (2014) 470–475.
- [32] T. Di Palma, F. Migliardini, D. Caputo, P. Corbo, *Carbohydr. Polym.* 157 (2017) 122–127.
- [33] F. Migliardini, T. Di Palma, M. Gaele, P. Corbo, *J. Solid State Electrochem.* 22 (2018) 2901–2916.
- [34] T. Di Palma, F. Migliardini, M. Gaele, P. Corbo, *Ionics* 25 (2019) 4209–4217.
- [35] P. Sun, J. Chen, Y. Huang, J.-H. Tian, S. Li, G. Wang, Q. Zhang, Z. Tian, L. Zhang, *Energy Storage Materials* 34 (2021) 427–435.
- [36] Y. Zuo, Y. Yu, H. Liu, Z. Gu, Q. Cao, C. Zuo, *Batteries* 6 (2020) 19.
- [37] Y. Wang, H.Y. Kwok, W. Pan, H. Zhang, X. Lu, D.Y. Leung, *Appl. Energy* 251 (2019) 113342.
- [38] J. Ren, C. Fu, Q. Dong, M. Jiang, A. Dong, G. Zhu, J. Zhang, B. Sun, *ACS Sustain. Chem. Eng.* (2021).
- [39] G. Wu, S. Lin, C. Yang, *J. Membr. Sci.* 280 (2006) 802–808.
- [40] A. Mohamad, *Corrosion Sci.* 50 (2008) 3475–3479.
- [41] W. Fang-Hui, L. Chun-Xi, M. Hong, W. Zi-Hao, *J. Beijing Univ. Chem. Technol.* 33 (2006) 17.
- [42] S. Luo, Y. Wang, T.C. Kong, W. Pan, X. Zhao, D.Y. Leung, *J. Power Sources* 490 (2021) 229526.
- [43] Y. Wang, H.Y. Kwok, W. Pan, Y. Zhang, H. Zhang, X. Lu, D.Y. Leung, *J. Power Sources* 450 (2020) 227685.